

Electrical resistivity surveys and data interpretation

Encyclopedia of Solid Earth Geophysics, 2nd Edition
Harsh Gupta et al. (eds.)
Springer

M.H.Loke¹, D. F. Rucker², J.E. Chambers³, P.B.Wilkinson³ and O. Kuras³

¹Geotomo Software Sdn. Bhd.
115, Cangkat Minden Jalan 5, Minden Heights,
Gelugor, 11700 Penang,
Malaysia
Email : drmhloke@yahoo.com
Tel : +60 4 6682920

²hydroGEOPHYSICS, Inc.
2302 North Forbes Boulevard
Tucson, AZ 85745,
USA
Tel : +1 520.647.3315

³ Geophysical Tomography Team
British Geological Survey
Keyworth
Nottingham NG12 5GG
UK
Email : jecha@bgs.ac.uk, pbw@bgs.ac.uk, oku@bgs.ac.uk
Tel : +44 (0)115 936 3100
Fax : +44 (0)115 936 3200

ELECTRICAL RESISTIVITY SURVEYS AND DATA INTERPRETATION

Definition

Electrical survey - Mapping the subsurface resistivity by injecting an electric current into the ground.

Electrode - Commonly a metal rod through which current is injected into the ground, or is used to measure the induced voltage on the ground surface.

Least-squares resistivity inversion - Finding the subsurface resistivity model that minimizes the sum of squares of the differences between the measured and calculated apparent resistivity values.

Introduction

Electrical resistivity surveys map the subsurface structure by making electrical measurements near the ground surface. An electric current is injected into the ground through two electrodes and the voltage difference is measured between two other electrodes (Figure 1a). The true subsurface resistivity can be estimated by making the measurements of potential difference at different positions of the current and potential electrodes, converting these values into apparent resistivity and then inverting the data set. The ground resistivity is related to various geological parameters such as the mineral and fluid content, porosity and degree of water saturation in the rock (*Electrical properties of rocks*). Over the past 25 years the resistivity method has undergone rapid developments in instrumentation, field survey techniques, data interpretation and novel applications in the geosciences. It has now become one of the standard geophysical exploration techniques widely used in environmental, engineering, hydrogeological and mining investigations.

The basic data from a resistivity survey are the positions of the current and potential electrodes, the current (I) injected into the ground and the resulting voltage difference (ΔV) between the potential electrodes (Figure 1a). The current and voltage measurements are then converted into apparent resistivity (*Instrumentation, electrical resistivity*), ρ_a , by using the following formula

$$\rho_a = k \frac{\Delta V}{I}, \quad (1)$$

where k is the geometric factor that depends on the configuration of the current and potential electrodes (Koefoed, 1979). Over the years, various electrode configurations (or arrays) have been developed. Figure 1 shows the arrangements for some commonly used arrays. A

discussion on the merits of the different arrays are given by Dahlin and Zhou (2004), Szalai and Szarka (2008) and Martorana et al. (2017). There has also been substantial work in nontraditional arrays that maximizes resolution of the subsurface (Wilkinson et al., 2013) or maximizes the use of unused channels on multi-channel resistivity meters (Cubbage et al., 2017). Determining the true subsurface resistivity from the apparent resistivity values is the data inversion problem.

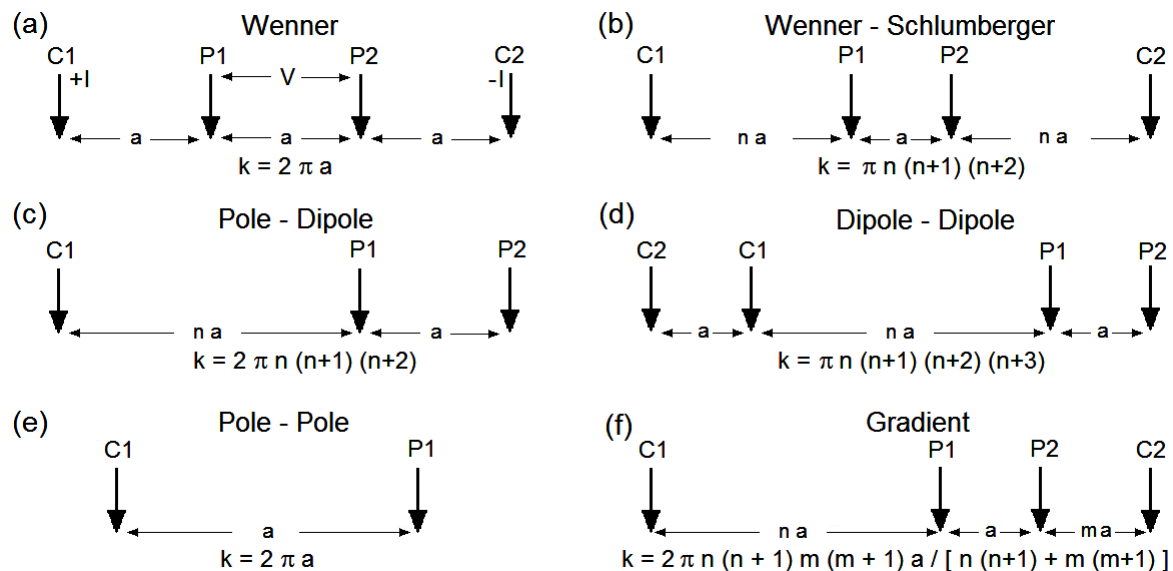


Figure 1. Common arrays used in resistivity surveys and their geometric factors. The current is injected into the ground through the C1 and C2 electrodes while the voltage difference is measured between the P1 and P2 electrodes. For the arrays with fewer than four electrodes, the remaining electrodes are placed at sufficiently large distances so that they do not affect the measurements.

Traditional profiling and sounding surveys

The resistivity survey method has its origin in the 1910s due to the work of the Schlumberger brothers. Traditionally resistivity surveys were divided into profiling and sounding surveys. The distances between the electrodes are kept fixed in a profiling survey, such as in the Wenner survey (Figure 1a), and the four electrodes are moved along the survey line. The data interpretation for profiling surveys was mainly qualitative. The second type of survey is the vertical sounding method, such as with the Schlumberger array (Figure 1b), where the center point of the electrode array remains fixed but the spacing between the electrodes is increased to obtain deeper subsurface information. Apparent resistivity plotted as a function of the current electrode spacing gives information on subsurface resistivity variations (Figure 2a).

Quantitative data interpretation for sounding surveys uses a one-dimensional (1-D) earth model with a series of horizontal layers (Figure 2b). One commonly used method for 1-D data inversion is the damped least-squares method (*Inverse theory, linear*) (Inman, 1975) that is based on the following equation

$$[\mathbf{J}_i^T \mathbf{J}_i + \lambda_i \mathbf{I}] \Delta \mathbf{q}_i = \mathbf{J}_i^T \mathbf{g}_i, \quad (2)$$

where the discrepancy vector $\Delta \mathbf{g}$ contains the difference between the logarithms of the measured and the calculated apparent resistivity values and $\Delta \mathbf{q}$ is a vector consisting of the deviation of the estimated model parameters from the true model. Here, the model parameters are the logarithms of the resistivity and thickness of the model layers. \mathbf{J} is the Jacobian matrix of partial derivatives of apparent resistivity with respect to the model parameters. i represents the iteration number. λ is a damping or regularization factor (Inman, 1975) that stabilizes the ill-conditioned Jacobian matrix usually encountered for geophysical problems (*Inverse theory, singular value decomposition*). Starting from an initial model (such as a homogeneous earth model), this method iteratively refines the model so as to reduce the data misfit to a desired level.

The resistivity sounding method has been used for many years, particularly in groundwater exploration. It gives useful results for subsurface features (such the water-table) where a 1-D model is an acceptable approximation. The greatest limitation of this method is that it does not take into account lateral changes in the subsurface resistivity which can result in errors in the interpreted resistivity and thicknesses of the layers. A two-dimensional (2-D) survey and interpretation model is required for more accurate results.

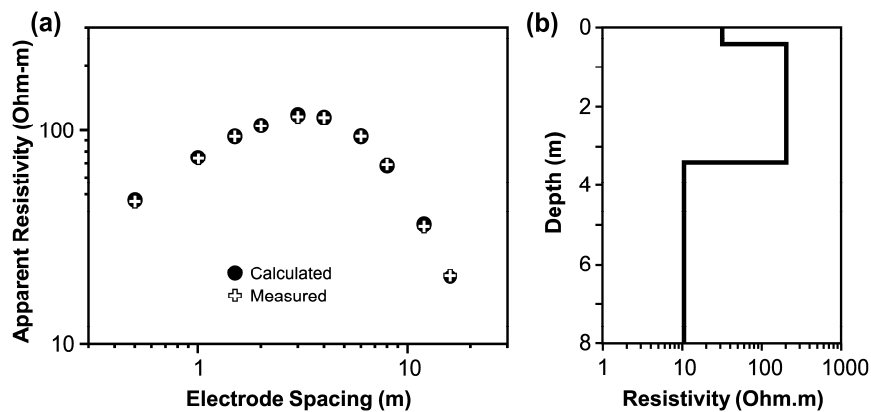


Figure 2. Example of (a) 1-D sounding curve and (b) layered earth model.

Two-dimensional resistivity imaging surveys

Since the early 1990s, development of the multi-electrode resistivity meter system (*Instrumentation, electrical resistivity*) has made 2-D surveys a practical tool for mapping moderately complex geological environments. The apparent resistivity measurements from the survey are commonly plotted in the form of a pseudosection (Edwards, 1977). The pseudosection (Figure 3a) is a useful method to present the data in a pictorial form and as an initial guide for further quantitative interpretation. The pseudosection gives a distorted picture of the subsurface because the shapes of the contours depend on the type of array used as well as the true subsurface resistivity.

A 2-D model that consists of a large number of cells is commonly used to interpret the data (Loke and Barker, 1996a). The finite-difference (*Numerical method, finite difference*) or finite-element methods (*Numerical method, finite element*) are used to calculate the apparent resistivity values for the 2-D model. A non-linear optimization method is then used to automatically change the resistivity of the model cells, so as to minimize the difference between the measured and calculated apparent resistivity values. The inversion problem is frequently ill-posed due to incomplete, inconsistent and noisy data. Smoothness or other constraints are usually incorporated to stabilize the inversion procedure such that numerical artifacts are avoided. As an example, the following equation includes a model smoothness constraint to the least-squares optimization method,

$$\left[\mathbf{J}_i^T \mathbf{R}_d \mathbf{J}_i + \lambda_i \mathbf{W}^T \mathbf{R}_m \mathbf{W} \right] \Delta \mathbf{q}_i = \mathbf{J}_i^T \mathbf{R}_d \mathbf{g}_i - \lambda_i \mathbf{W}^T \mathbf{R}_m \mathbf{W} \mathbf{q}_{i-1}. \quad (3)$$

\mathbf{W} includes the roughness filters in the x-, y- and z- directions. \mathbf{R}_d and \mathbf{R}_m are weighting matrices employed if the L1-norm inversion method is used (Farquharson and Oldenburg, 1998; Loke *et al.*, 2003). One common form of the roughness filter is the first-order difference matrix (deGroot-Hedlin and Constable, 1990), but the elements of the matrices can be modified to introduce other desired characteristics into the inversion model (Pellerin and Wannamaker, 2005; Farquharson, 2008). The method can also be modified to produce 'blocky' models for regions that are piecewise constant and separated by sharp boundaries (Farquharson and Oldenburg, 1998; Loke *et al.*, 2003). A number of computer-based software packages are now available that can automatically carry out the inversion of a 2-D survey data set in seconds.

Figure 3a shows an example of a measured apparent resistivity pseudosection from a survey using the dipole-dipole array. The resistivity model after inversion is shown in Figure 3b. This survey was part of a long-term landslide monitoring program. From the base to the top of the slope, the formations are the Lias Group Redcar Mudstone Formation (RMF), Staithes Sandstone and Cleveland Ironstone Formation (SSF), and Whitby Mudstone Formation (WMF). Slope failure occurs within the WMF in the upper parts of the slope (Uhlemann *et al.*, 2017).

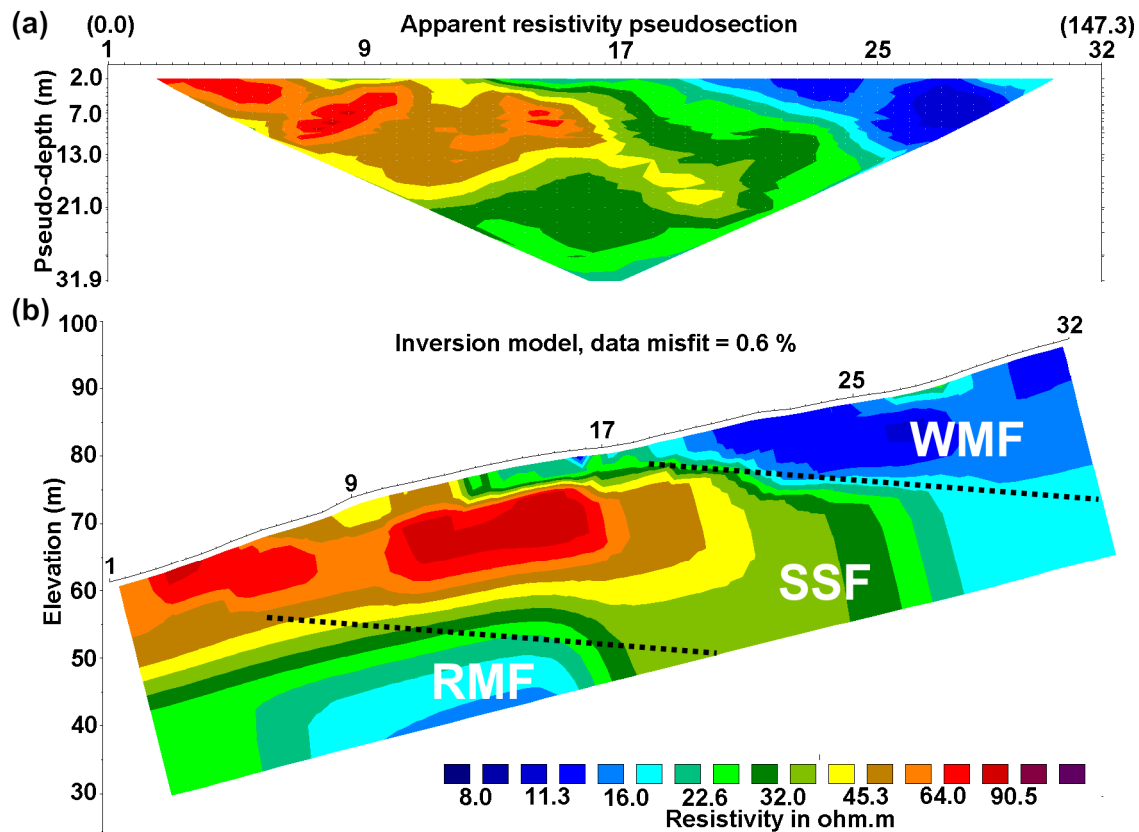


Figure 3. Example of (a) apparent resistivity pseudosection and (b) 2-D inverse model.

Three-dimensional resistivity imaging surveys

Since geological structures tend to be three-dimensional (3-D) in nature, a 3-D resistivity survey and interpretation model (Figure 4) should give the most accurate results. Although it has not reached the same level of usage as 2-D surveys, it is now more widely used in very complex areas such as in many environmental (Chambers *et al.*, 2006; Rucker *et al.*, 2010) and mineral exploration surveys (White *et al.*, 2001; Bingham *et al.*, 2006; Abbassi *et al.*, 2018). Many of the early 3-D surveys used the pole-pole array over relatively small grids (up to about 20 by 20 electrodes) with measurements in different directions (Park and Van, 1991;

Loke and Barker, 1996b). The use of other arrays, such as the pole-dipole and Wenner-Schlumberger, is now becoming more common in 3-D surveys that involve thousands of electrode positions (White et al., 2001; Chambers et al., 2006). A true 3-D survey requires placing of electrodes in the form of a 3-D grid. However, a more cost-effective strategy is usually followed wherein 3-D data sets are collated from independent 2-D survey lines. This strategy greatly reduces the cost of a 3-D survey and also allows for 2-D inversions of each individual line. The data interpretation techniques used for 2-D surveys can be extended to 3-D surveys (Loke and Barker, 1996b). Fast computer software that takes minutes to hours to invert a 3-D data set (depending on size) on multi-core PCs is now available (Loke et al., 2013). Other non-linear optimization methods such as neural networks, simulated annealing and conjugate gradient techniques have also been used for resistivity data inversion (Pellerin and Wannamaker, 2005).

Figure 4 shows an example from the Hanford site in Washington state, USA where liquid waste of high ionic strength (mostly comprised of sodium nitrate) was disposed in trenches and concrete cribs (Rucker et al., 2009). Different resistivity survey phases were carried out using 2-D lines in different directions and with different spacings. The linear high resistivity features near the surface are due to the trenches and concrete cribs. The leakage zones are marked by the prominent low resistivity zones in the deeper regions.

The field survey and data inversion methods have been adapted for other types of problems such induced polarization (IP) surveys (White et al., 2001; Fiandaca et al., 2013), measurements across boreholes (Wilkinson et al., 2008), aquatic surveys (Rucker and Noonan, 2013; Dahlin and Loke, 2018), for cylindrical geometries (Chambers et al., 2004; al Hagrey et al., 2004), measurements with long electrodes (Rucker et al., 2010; Ronczka et al., 2015) and mobile survey systems (*Instrumentation, electrical resistivity*).

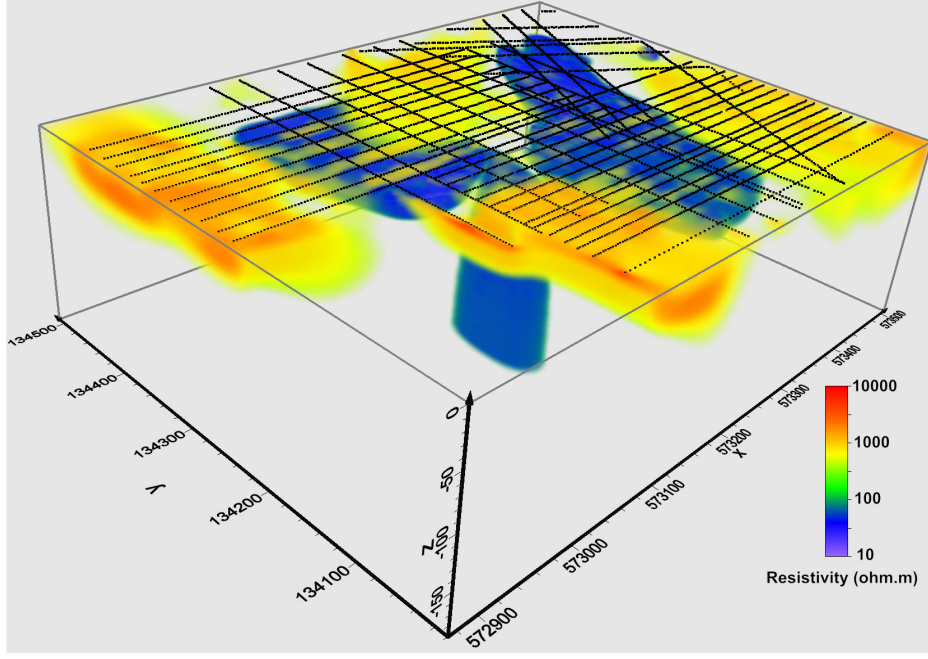


Figure 4. A 3-D survey (electrodes marked by black dots) and model. Blue regions have resistivity of less than 100 ohm.m, while light-green and orange regions have resistivity above 400 ohm.m.

4-D time-lapse surveys

In time-lapse surveys measurements using the same array configurations are repeated, usually at regular intervals, to monitor temporal changes in the subsurface resistivity. The least-squares optimization method can be modified for time-lapse surveys so as to minimize temporal changes in the model resistivity values (Kim et al., 2009; Loke et al., 2014), as shown by the following equation.

$$\left[\mathbf{J}_i^T \mathbf{R}_d \mathbf{J}_i + (\lambda_i \mathbf{W}^T \mathbf{R}_m \mathbf{W} + \alpha_i \mathbf{M}^T \mathbf{R}_t \mathbf{M}) \right] \Delta \mathbf{q}_i = \mathbf{J}_i^T \mathbf{R}_d \mathbf{g}_i - (\lambda_i \mathbf{W}^T \mathbf{R}_m \mathbf{W} + \alpha_i \mathbf{M}^T \mathbf{R}_t \mathbf{M}) \mathbf{q}_{i-1} \quad (4)$$

\mathbf{M} is a difference matrix applied across the time models to minimize the difference in the resistivity of each model cell and the corresponding cell for the next temporal model.

Sophisticated integrated monitoring data acquisition systems have been developed in recent years (Rosquist *et al.*, 2011; Uhlemann *et al.*, 2017; Poje *et al.*, 2018) that can automatically carry out the measurements at preset times and transmit the data over the internet to a processing center where it is automatically inverted. Figure 5 shows an example from a survey to monitor the flow of a leaching reagent through a rock ore heap as part of a secondary recovery method at a gold mine (Rucker *et al.*, 2014; Poje *et al.*, 2018). Plots of the change in saturation (calculated from the change in the resistivity) show the regions

within the rock heap penetrated by the leaching reagent. The volumes of the regions covered by the plumes provided an estimate of the value of the gold and silver extracted using the known concentration of the metals.

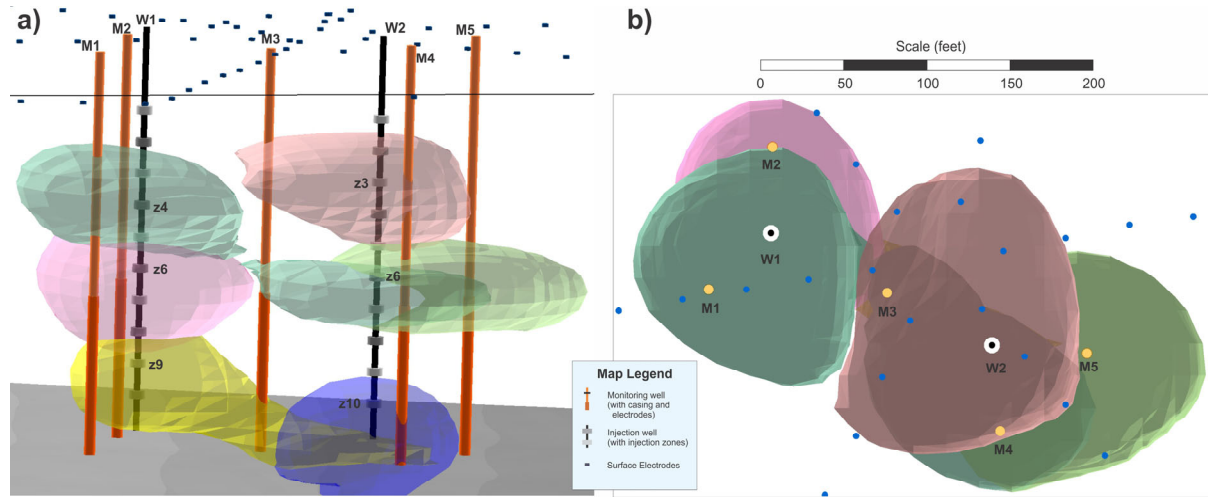


Figure 5. Stacked plumes of 5% saturation increase for different zones from injects at wells W1 and W2 (a) side view; and (b) overhead view.

Summary

The electrical resistivity survey method has undergone tremendous changes over the past 25 years. While traditional resistivity profiling and sounding surveys are still used, 2-D imaging surveys are now the method of choice for most areas as they can accurately map moderately complex structures. The field equipment and computer interpretation software are widely available. 3-D surveys now play an increasingly important role in very complex areas. In many cases the 3-D data set is collated from a number of separate 2-D survey lines. There have been rapid developments within the past decade in the instrumentation, data acquisition and inverse modelling techniques for 4-D time-lapse surveys to monitor temporal changes in the subsurface resistivity.

Acknowledgements

Chambers, Wilkinson and Kuras publish with the permission of the Executive Director, British Geological Survey (UKRI-NERC)

Dale – any, such as to AngloGold for the field example? None for me. The figure was from an independent gold mine in Nevada that would like to remain anonymous.

Bibliography

- Abbassi, B., Cheng, L.Z., Richards, J.P., Hübert, J., Legault, J.M., Rebagliati, M. and Witherly, K., 2018. Geophysical properties of an epithermal Au-Ag deposit in British Columbia, Canada. *Interpretation*, 6(4): T907-T918.
- al Hagrey, S.A., Meissner, R., Werban, U., Rabbel, W. and Ismaeil, A., 2004. Hydro-, bio-geophysics. *The Leading Edge*, 23: 670-674.
- Bingham, D., Nimeck, G., Wood, G. and Mathieson, T., 2006. 3D resistivity in the Athabasca basin with the pole-pole array. In *Geophysical methods and techniques applied to uranium exploration workshop proceedings*. SEG Annual General Meeting 2006, New Orleans.
- Chambers, J.E, Loke, M.H., Ogilvy, R.D. and Meldrum, P.I., 2004. Non-invasive monitoring of DNAPL migration through a saturated porous medium using electrical impedance tomography. *Journal of Contaminant Hydrology*, 68: 1-22.
- Chambers, J.E., Kuras, O., Meldrum, P.I., Ogilvy, R.D. and Hollands, J., 2006. Electrical resistivity tomography applied to geologic, hydrogeologic, and engineering investigations at a former waste-disposal site. *Geophysics*, 71: B231-B239.
- Cabbage, B., Noonan, G.E. and Rucker, D.F., 2017. A Modified Wenner Array for Efficient Use of Eight-Channel Resistivity Meters. *Pure and Applied Geophysics*, 174: 2705-2718.
- Dahlin, T. and Zhou, B., 2004, A numerical comparison of 2D resistivity imaging with ten electrode arrays. *Geophysical Prospecting*, 52: 379-398.
- Dahlin, T. and Loke, M.H., 2018. Underwater ERT surveying in water with resistivity layering with example of application to site investigation for a rock tunnel in central Stockholm. *Near Surface Geophysics*, 16: 230-237.
- deGroot-Hedlin, C. and Constable, S., 1990. Occam's inversion to generate smooth, two-dimensional models from magnetotelluric data. *Geophysics*, 55: 1613-1624.
- Edwards L.S., 1977. A modified pseudosection for resistivity and induced-polarization. *Geophysics*, 42: 1020-1036.
- Farquharson, C.G., and D.W. Oldenburg, 1998. Nonlinear inversion using general measures of data misfit and model structure. *Geophysical Journal International*, 134: 213-227.
- Farquharson, C.G., 2008. Constructing piecewise-constant models in multidimensional minimum-structure inversions. *Geophysics*, 73: K1-K9.
- Fiandaca, G., Ramm, J., Binley, A., Gazoty, A, Christiansen, A.V., Auken, E., 2013. Resolving spectral information from time domain induced polarization data through 2-D inversion. *Geophysical Journal International*, 192: 631–646.
- Inman, J.R., 1975. Resistivity inversion with ridge regression. *Geophysics*, 40: 798-817.
- Koefoed, O., 1979. *Geosounding Principles 1 : Resistivity sounding measurements*. Amsterdam: Elsevier Science Publishing Company.
- Kim, J H., M J. Yi, S G., Park, and J.G. Kim, 2009. 4D inversion of DC resistivity monitoring data acquired over a dynamically changing earth model. *Journal of Applied Geophysics*, 68:522-532.
- Loke, M.H. and Barker, R.D., 1996a. Rapid least-squares inversion of apparent resistivity pseudosections using a quasi-Newton method. *Geophysical Prospecting*, 44: 131-152.

- Loke, M.H. and Barker, R.D., 1996b. Practical techniques for 3D resistivity surveys and data inversion. Geophysical Prospecting, 44: 499-523.
- Loke, M.H., Acworth, I. and Dahlin, T., 2003. A comparison of smooth and blocky inversion methods in 2D electrical imaging surveys. Exploration Geophysics, 34: 182-187.
- Loke, M.H., Chambers, J.E., Rucker, D. F., Kuras, O. and Wilkinson, P. B., 2013. Recent developments in the direct-current geoelectrical imaging method. Journal of Applied Geophysics , 95: 135-156.
- Loke, M.H., Dahlin, T., Rucker, D.F., 2014. Smoothness-constrained time-lapse inversion of data from 3-D resistivity surveys. Near Surface Geophysics, 12: 5-24.
- Martorana, R., Capizzi, P., D'Alessandro, A. and Luzio, D. 2017. Comparison of different sets of array configurations for multichannel 2D ERT acquisition. Journal of Applied Geophysics, 137: 34-48.
- Park, S.K. and Van, G.P., 1991. Inversion of pole-pole data for 3-D resistivity structures beneath arrays of electrodes. Geophysics, 56: 951-960.
- Pellerin, L and Wannamaker, P.E., 2005. Multi-dimensional electromagnetic modeling and inversion with application to near-surface earth investigations. Computers and Electronics in Agriculture, 46: 71-102.
- Poje, M., Salgado, L., Rucker, D.F., Levitt, M., Strohmeyer, J., McNeill, M., Rucker, K., Berumen, R. and Galbraith, H., 2018. Optimizing Gold Leaching with the Aid of Electrical Resistivity Geophysics. Fast Times, 23(2): 62-68.
- Ronzka, M., Rucker, C. and Günther, T., 2015. Numerical study of long-electrode electric resistivity tomography-Accuracy, sensitivity, and resolution. Geophysics, 80: E317-E328.
- Rosquist, H., Leroux, V., Dahlin, T., Svensson, M., Lindsjö, M., Månsson, C-H. and Johansson, S., 2011. Mapping landfill gas migration using resistivity monitoring. Waste and Resource Management, 164(1): 3-15.
- Rucker, D.F., Levin, M.T. and Myers, D.A., 2007. Imaging beneath Hanford's Tank Farms with electrical resistivity geophysics - An innovative approach. WM '07 Conference, Feb. 25-March 1, 2007, Tuscon, AZ.
- Rucker, D., Loke, M.H., Levitt, M.T. and Noonan, G.E., 2010. Electrical resistivity characterization of an industrial site using long electrodes. Geophysics , 75: WA95-WA104.
- Rucker, D.F., Levitt, M.T. and Greenwood, W.J., 2009. Three-dimensional electrical resistivity model of a nuclear waste disposal site. Journal of Applied Geophysics, 69: 150-164.
- Rucker, D.F. and Noonan, G.E., 2013. Using marine resistivity to map geotechnical properties: a case study in support of dredging the Panama Canal. Near Surface Geophysics, 11: 625-637.
- Rucker, D.F, Crook, N., Winterton, J., McNeill, M., Baldyga, C.A., Noonan, G. and Fink, J.B., 2014. Real-time electrical monitoring of reagent delivery during a subsurface amendment experiment. Near Surface Geophysics, 12: 151-163.
- Szalai, S., Szarka, L., 2008. On the classification of surface geoelectric arrays. Geophysical Prospecting, 56: 159-175.
- Uhlemann, S., Chambers, J., Wilkinson, P., Maurer, H., Merritt, A., Meldrum, P., Kuras, O., Gunn, D., Smith, A. and Dijkstra, T., 2017. Four-dimensional imaging of moisture dynamics during landslide reactivation. Journal of Geophysical Research : Earth

Surface, 122(1):398-418.

White, R.M.S., Collins, S., Denne, R., Hee, R. and Brown, P., 2001. A new survey design for 3D IP modelling at Copper hill. Exploration Geophysics, 32: 152-155.

Wilkinson, P. B., Chambers, J. E., Lelliott, M., Wealthall P. and Ogilvy, R. D., 2008. Extreme sensitivity of crosshole electrical resistivity tomography measurements to geometric errors. Geophysical Journal International, 173: 49-62.

Wilkinson, P.B., Loke, M.H., Meldrum, P.I., Chambers, J.E., Kuras, O., Gunn, D.A. and Ogilvy, R.D., 2012. Practical aspects of applied optimised survey design for Electrical Resistivity Tomography. Geophysical Journal International, 189: 428-440.

Cross-References

- Electrical properties of rocks
- Instrumentation, electrical resistivity
- Inverse theory, linear
- Inverse theory, singular value decomposition
- Numerical method, finite difference
- Numerical method, finite element